AJNR Am J Neuroradiol 23:393–399, March 2002

Influence of Imaging Parameters on High-Intensity Cerebrospinal Fluid Artifacts in Fast-FLAIR MR Imaging

Hsiu-Mei Wu, David M. Yousem, Hsiao-Wen Chung, Wan-Yuo Guo, Cheng-Yen Chang, and Cheng-Yu Chen

BACKGROUND AND PURPOSE: **High-intensity CSF artifacts at the basal cisterns on MR images are often seen when a fast fluid-attenuated inversion recovery (FLAIR) technique is used. We investigated the influences of four optional fast-FLAIR sequence parameters on the high-intensity CSF artifacts.**

METHODS: **A total of 377 patients (age range, 1 week to 91 years; mean 40.6 years; 186 female, 191 male) were examined with axial fast-FLAIR images obtained ($TR/TE_{eff}/TI$, 8800/133/2200) with a 1.5-T system during 6 months. The effects of the optional addition of inferior inflow saturation (thickness, 80 mm), section flow compensation, and tailored radiofrequency (TRF) pulses, plus the choice of interleaving acquisition factors of 2 or 3, were evaluated for the presence of high-intensity CSF artifacts on the fast-FLAIR images. Two radiologists independently reviewed the fast-FLAIR images in 76 patients; afterward, a single observer reviewed the remainder of the images.**

RESULTS: **The interobserver agreement rate in 76 cases was more than 90%. The use of TRF and/or three interleaving acquisitions resulted in a substantial reduction in the incidence of high-intensity CSF artifacts from about 80% to 40% ($P < .05$, two-sample two-sided Z test). Inferior inflow saturation and section flow compensation did not significantly improve image quality ($P > .05$). The results were consistent with the image quality ranking obtained in five healthy volunteers.**

CONCLUSION: **The appropriate choice of sequence parameters in fast-FLAIR imaging reduces the incidence of high-intensity CSF artifacts that are frequently encountered in the presence of rapid CSF flow.**

The advent of fluid-attenuated inversion recovery (FLAIR) imaging has improved the detection of intraparenchymal abnormalities in the brain by highlighting hyperintense lesions opposite the low-signal-intensity CSF (1–3). Because of the conspicuous lesion contrast, the FLAIR sequence has become a staple in the evaluation of intracranial pathologic conditions (4–7). In particular, the incorporation of fast spin-echo imaging to FLAIR imaging, the so-called fast-FLAIR technique (8, 9), has made the use of this method feasible in clinical practice because of a substantial reduction in the imaging time. Findings from recent studies suggest that the fast-FLAIR images can be used to detect diseases within the subarachnoid space, such as subarachnoid hemorrhage (5, 10), meningitis (7, 9), and subarachnoid seeding of neoplasms (7). Consequently, an integrated MR examination including FLAIR and MR angiography would be helpful for the examination of patients with possible subarachnoid hemorrhage, as well as different types of aneurysms.

Despite the relative success of the fast-FLAIR technique in lesion detection within the convexity of the subarachnoid space, CSF suppression with fast-FLAIR at the basal cisterns is less successful. Artifactual high signal intensity can often be found in the

Received July 10, 2001; accepted after revision November 6.

From the Department of Radiology (H.M.W., D.M.Y.), Johns Hopkins University, Baltimore, MD; the Department of Radiology (H.-M.W., W.-Y.G., C.-Y. Chang), Veterans General Hospital-Taipei, Taiwan, ROC; the Department of Radiology (H.-M.W., W.-Y.G., C.-Y. Chang.), School of Medicine, National Yang-Ming University, Taipei, Taiwan, ROC; the Department of Electrical Engineering (H.-W.C.), National Taiwan University, Taipei, Taiwan, ROC; the Department of Radiology (H.-W.C, C.-Y. Chen.), Tri-Service General Hospital, Nei-Hu, Taipei, Taiwan, ROC.

H.-M.W. received support from Tjing-Ling Neurological Foundation. H.-W.C. received support from the National Science Council, grant NSC90–2320-B002–043-M08.

Address reprint requests to Hsui-Mei Wu, MD, Department of Radiology, Veterans General Hospital-Taipei, No. 201, Section 2, Shih-Pai Road, Taipei, Taiwan 112, ROC.

TABLE 1: Incidence of high-intensity CSF artifacts at the basal cisterns in image groups classified according to combinations of pulse sequence parameters

Parameters*	Mean Patient Age (y)	No. of Patients	No. with High-Intensity CSF Artifacts at the Basal Cisterns	Incidence (%)
+FC/+TRF/2/−I sat	42.3	84	36	42.9
+FC/+TRF/2/+I sat	43.6	39	18	46.2
−FC/−TRF/2/+I sat	41.4	104	72	69.2
−FC/−TRF/2/−I sat	38.2	32	26	81.3
−FC/−TRF/3/+I sat	35.6	48	22	45.8
−FC/+TRF/2/+I sat	44.8	27	12	44.4
+FC/−TRF/2/−I sat	37.4	43	32	74.4

* +FC indicates with FC along section direction; −FC, without FC; +I sat, with inferior inflow saturation; −I sat, without inferior inflow saturation; +TRF, with TRF pulses; −TRF, without TRF pulses; and 2 or 3, the interleaving acquisition factor.

prepontine and perimesencephalic regions (3, 8, 11), and the diagnosis of focal subarachnoid hemorrhage at these locations becomes difficult, if not impossible. Therefore, the purpose of this study was to investigate the effects of various imaging parameters on fast-FLAIR high-intensity CSF artifacts at the basal cisterns. The incidence of high-intensity CSF artifacts for each set of sequence parameter combinations was also determined.

Methods

A total of 377 individuals (age range, one week to 91 years; 186 females with a mean age of 40 years, 191 males with a mean age of 41 years) were examined with a 1.5-T MR system during a 6-month period. We excluded patients who had undergone intracranial surgery within 6 months prior to the date of the imaging examination to eliminate the influence of meningeal pathologic conditions on the evaluation of fast-FLAIR performance. In addition, all patient records were reviewed to ensure that, if lumbar punctures were performed, the findings were normal.

Axial fast-FLAIR images were acquired by using a standard quadrature head coil with the following imaging parameters: $TR/TE_{eff}/TI$ of 8800/133/2200, readout bandwidth 16 kHz, one NEX, 192 × 256 matrix, 22 × 22 or 24 × 24-cm field of view, and 5-mm section thickness with interleaved images (two acquisitions). All images were reconstructed by using a zero-filling interpolation process to a display matrix of 512 × 512 to enhance the apparent image resolution. Four pulse sequence parameters that were thought to potentially affect the extent of high-intensity CSF artifacts on fast-FLAIR images were varied, and their effects on the imaging appearance was investigated. The changes included the optional addition of the following: 1) inferior inflow saturation with a thickness of 80 mm, which could potentially suppress signals from through-plane inflow of CSF; 2) flow compensation (FC) along the section direction, which was thought to affect the degree of intravoxel phase dispersion due to CSF motion in the presence of imaging gradients; 3) tailored radiofrequency (TRF) pulses in an echo-amplitude stabilization scheme with flip-angle adjustment in a fast spin-echo sequence (12); and 4) an interleaving acquisition factor of 2 (manufacturer's default) or 3. Here, the interleaving acquisition factor specifically represented the number of image-acquisition passages for whole-brain coverage. For example, by choosing an interleaving acquisition factor of 3, imaging was divided into three steps; during each, mutually adjacent images were acquired with a section gap of twice the section thickness. The theoretical basis of the above four parameters related to high-intensity CSF artifacts are further addressed in the Discussion.

These parameters were changed on a weekly basis during the 6-month period to achieve sufficient statistical power to evaluate the parameter effects. Note that we did not change all of the parameters in any single patient; instead, we chose to evaluate a cohort of patients with each set of parameter combinations. In addition, not all combinations of the four parameters were investigated for two reasons: First, because of the imaging time, the interleaving factor of 3 was not the preferred choice. Thus, we did not specifically use the interleaving factor of 3 with all possible combinations of the other parameters. Second, some parameters that were found during the investigation to minimally affect the incidence of high-intensity CSF artifacts were subsequently fixed in later cases. Therefore, the total number of combinations investigated in this study was seven (Table 1). Also, the effect of cardiac gating on high-intensity CSF artifacts was not investigated, for reasons stated in the Discussion.

The fast-FLAIR images were evaluated for the presence of high-intensity CSF artifacts in the subarachnoid space, especially the prepontine and perimesencephalic cisterns. The presence of high-intensity artifacts was defined as CSF with signal intensity higher than that of gray matter, either focally or diffusely. Although sagittal T1-weighted, axial fast spin-echo T2-weighted, axial T1-weighted, and contrast-enhanced axial T1-weighted images were acquired in most patients, these images were not routinely reviewed during the evaluation for fast-FLAIR artifacts. Two neuroradiologists (H.-M.W., D.M.Y.) initially interpreted the fast-FLAIR images to evaluate the interobserver variability in the analysis of high-intensity CSF artifacts in the perimesencephalic and prepontine regions. After the initial evaluation of the images in 76 patients, for which the agreement rate was greater than 90% (the interobserver agreement regarding the presence of high signal intensity in the basal cisterns was 93%), a single observer (H.-M.W.) reviewed the remaining images. The results obtained after the completion of all case reviews were subsequently divided into groups according to the combinations of the four sequence parameters being investigated. The statistical significance of differences in artifact incidences between the groups was assessed by using two-sample two-sided Z test.

In addition to the patient examinations, fast-FLAIR imaging with different combinations of pulse sequence parameters was performed in five healthy volunteers for an evaluation of image appearances in a subject-independent manner. In this part of the investigation, two neuroradiologists (H.-M.W., D.M.Y.) independently reviewed and ranked the presence of high-intensity CSF artifacts at the basal cisterns. Each neuroradiologist were blinded the pulse sequence parameters and the results of the other neuroradiologist. A final ranking of image quality for each subject was reached by consensus.

Results

Of the 377 patients whose images were reviewed, meningeal disease was suspected in none. According to the chosen pulse sequence parameters, the images

TABLE 2: Comparison of the incidence of high-intensity CSF artifacts at the basal cisterns between groups

Comparison of Parameters Changed*	Parameters Maintained*	*Z* Value	*P* Value	Significant Difference
+I sat vs −I sat	+FC/+TRF/2	0.148	.882	No
+I sat vs −I sat	−FC/−TRF/2	1.109	.268	No
2 vs 3	−FC/−TRF/+I sat	2.581	.010	Yes
+FC vs −FC	+TRF/2/+I sat	−0.114	.909	No
+FC vs −FC	−TRF/2/−I sat	0.420	.675	No
+TRF vs −TRF	+FC/2/−I sat	3.187	.001	Yes
+TRF vs −TRF	−FC/2/+I sat	2.168	.030	Yes
+FC/+TRF vs −FC/−TRF	2/+I sat	2.351	.019	Yes
+FC/+TRF vs −FC/−TRF	2/−I sat	3.530	<.001	Yes
+FC/+TRF/2/−I sat vs −FC/−TRF/3/+I sat	None	0.148	.882	No

* +FC indicates with FC along section direction; −FC, without FC; +I sat, with inferior inflow saturation; −I sat, without inferior inflow saturation; +TRF, with TRF pulses; −TRF, without TRF pulses; and 2 or 3, the interleaving acquisition factor.

TABLE 3: Ranking of image quality in five healthy volunteers*

Rank†	Volunteer 1	Volunteer 2	Volunteer 3	Volunteer 4	Volunteer 5
1	FC/TRF/3	FC/TRF/3	FC/TRF/3	FC/TRF/3	FC/TRF/3
2	TRF/2	FC/I-S sat/TRF/2	FC/I sat/TRF/2	TRF/2	TRF/2
3	FC/TRF/2	FC/I sat/TRF/2	FC/TRF/2	FC/I-S sat/TRF/2	FC/TRF/2
4	FC/I sat/TRF/2	FC/TRF/2	FC/I-S sat/TRF/2	FC/I sat/TRF/2	FC/I sat/TRF/2
5	FC/I-S sat/TRF/2	TRF/2	TRF/2	FC/TRF/2	FC/I-S sat/TRF/2
6	None/2	FC/2	None/2	None/2	None/2
7	FC/2	NA	FC/2	FC/2	FC/2
8	NA	NA	NA	NA	I-S sat/2

* FC indicates FC along section direction; I-S sat, with both inferior and superior inflow saturation; NA, not applicable; and 2 or 3, the interleaving acquisition factor.

† 1 indicates the least high-intensity CSF artifacts.

were divided into seven groups. Statistical analysis showed that the groups did not significantly differ in age and sex distribution. The incidences of high-intensity CSF artifacts at the basal cisterns in all groups are shown in Table 1. Note that the high-intensity CSF artifacts occurred with rates greater than 40% in all groups. With inappropriate choices of pulse sequence parameters (eg, no TRF, no FC, two acquisitions), however, the incidence of artifacts increased to about 80%. The fast-FLAIR images obtained without the TRF option seemed to yield a higher incidence of artifacts, unless an interleaving acquisition factor of 3 was used. Such consequences are evident in Table 2, which shows the statistical differences of artifact incidence between groups, as assessed by using the *Z* test. As Table 2 shows, the use of inferior inflow saturation and/or section flow compensation did not affect the incidence of high-intensity CSF artifacts. The use of TRF or an interleaving acquisition of 3 significantly reduced the high-intensity CSF artifacts at the basal cisterns. The presence of artifacts on images acquired with an interleaving acquisition factor of 3 without TRF pulses was not significantly different from those on images obtained by using an interleaving acquisition factor of 2 with the TRF option.

Results from the five volunteers demonstrated that the fast-FLAIR images obtained with section FC, TRF, and an interleaving acquisition factor of 3 consistently had the best image quality with the least high-intensity CSF artifacts at the basal cisterns (Table 3). The images acquired with TRF pulses and an interleaving acquisition factor of 2 were ranked as being slightly inferior to those obtained with TRF pulses and three interleaving acquisitions. Note that all fast-FLAIR imaging acquired with a TRF pulse and an interleaving acquisition factor of 2 were similar, even with different combinations of section FC, inferior inflow saturation, and/or superior inflow saturation (Fig 1). Hence, the rankings for these sequence parameter combinations were more or less interchangeable. Imaging without the TRF option always result in the worst high-intensity CSF artifacts.

Discussion

Imaging of the brain with the fast-FLAIR technique provides a unique advantage of high sensitivity to hemorrhage in the subarachnoid space (5, 7, 10). The existence of plasma protein shortens the T1 of the subarachnoid fluid (13); this leads to high signal intensity on the fast-FLAIR images of the hemorrhagic lesions opposing the low-signal CSF (3, 5, 7, 10). Consequently, previous groups have found that fast-FLAIR imaging is superior to CT scanning (5, 10), proton-density–weighted imaging, and T2-weighted imaging (8, 14) in demonstrating subarachnoid hemorrhage, particularly with subacute subarachnoid hemorrhage (15). In the presence of CSF motion, however, inflow of noninverted (and hence non-nullified) CSF into the imaging section is likely to

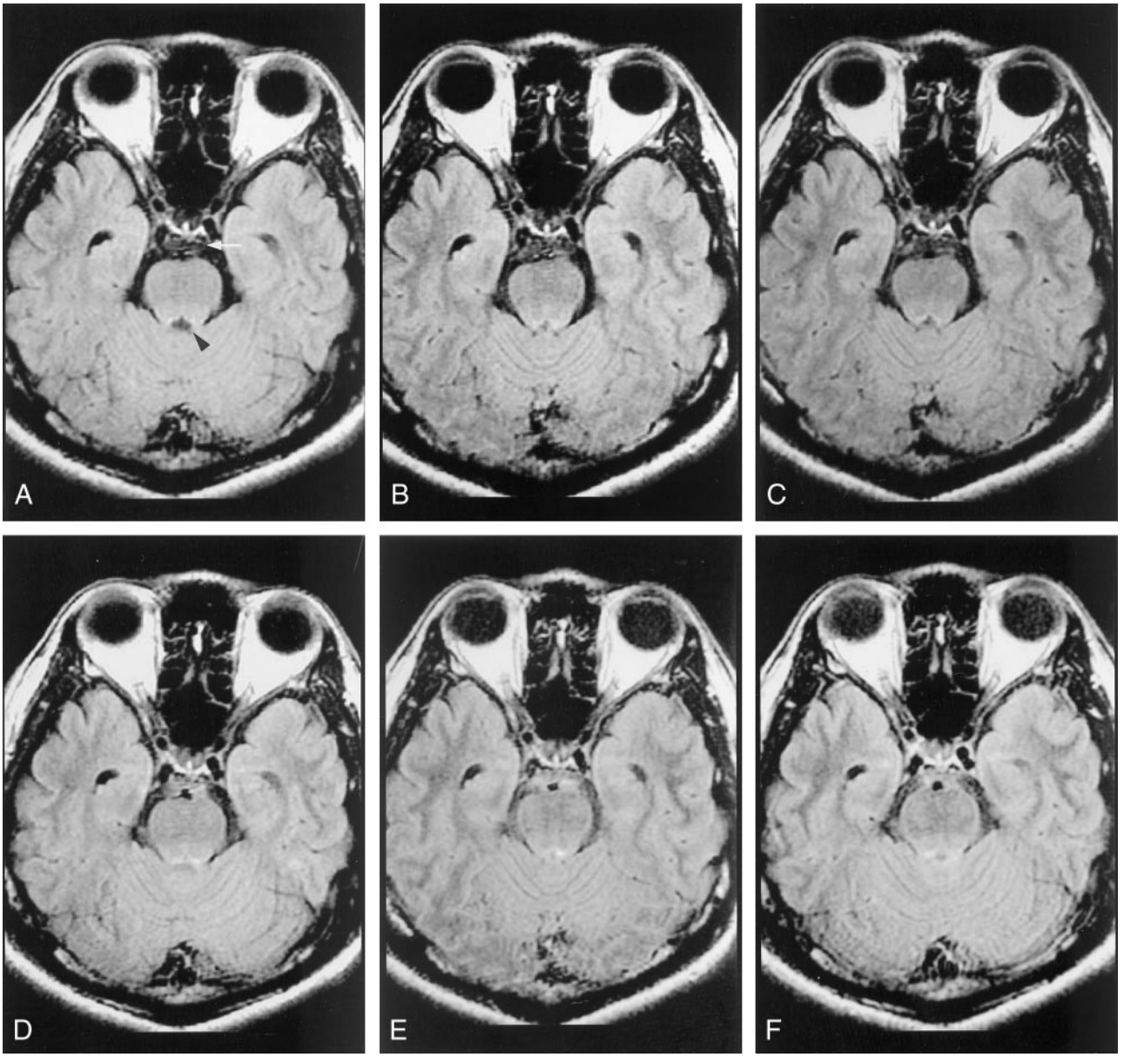

FIG 1. Comparison of images parameters in terms of high-intensity CSF artifacts on fast-FLAIR images obtained in a 37-year-old healthy male volunteer (volunteer 5).

A, Image obtained with section FC, TRF, and interleaving acquisition factor of 3 shows better CSF nulling at prepontine cistern (*arrow*) than the images in *B* or *C*. Notably, in pulse sequences with better CSF nulling at prepontine cistern, fewer high-intensity CSF artifacts are present at the aqueduct (*arrowhead*).

B, Image obtained with FC, TRF, and an interleaving acquisition factor of 2.

C, Image obtained with only TRF.

D, Additional superior and inferior presaturation does not decrease the high-intensity CSF artifacts (see image in *B*).

E and *F*, Images obtained with FC alone without TRF (*E*) or with superior and inferior presaturations (saturation bands of 80 mm) without TRF (*F*) demonstrate substantial high-intensity CSF artifacts at the prepontine cistern.

occur during the 2-second TI, particularly at places where fast pulsatile flows are present (3, 11). Such a phenomenon manifests as high-intensity CSF artifacts on fast-FLAIR images (1, 8), causing nonspecificity in hemorrhage detection and, possibly, motion ghosts that hamper accurate image interpretation (3, 16). Therefore, in addition to an optimization of standard imaging parameters such as the TR, TI, TE (17), and echo train length (18) toward effective CSF suppression, one should be cognizant of the various optional sequence parameters that can be chosen to eradicate the flow-related high-intensity CSF artifacts frequently encountered at the basal cisterns.

Of the four optional sequence parameters investigated in this study, inflow saturation and section FC did not significantly affect the incidence of high-intensity CSF artifacts. In principle, the application of inflow saturation presaturates the magnetization from upstream flow (usually in major blood vessels), thereby eliminating signals from the through-plane flowing fluid. For CSF at the basal cisterns, however, the flow is generally bidirectional (ie, to and fro), and

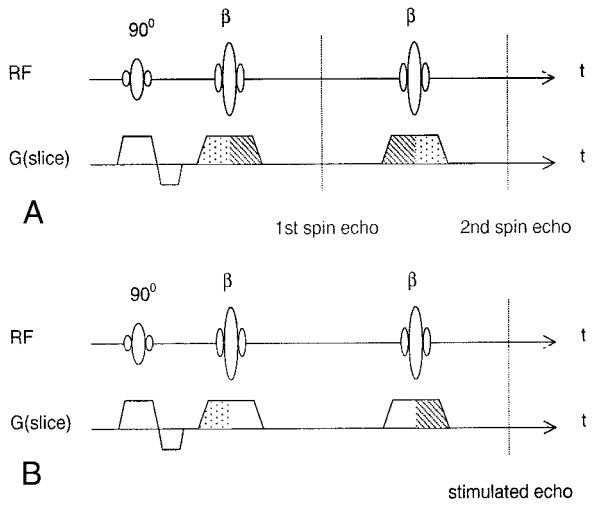

FIG 2. Schematic diagrams of the fast spin-echo sequence show the effects of section selection gradients on the formation of spin echoes and stimulated echoes.

A, Diagram shows the spin echoes produced with RF excitation by the 90° pulse and refocusing by the β pulses. At even echoes, the section selection gradient shows a 1-(-2)-1 waveform (dotted-dashed-dotted areas, respectively). Hence, the spin echoes are have inherent motion compensation at even echoes.

B, Diagram shows stimulated echo formation from RF excitation by the 90° pulse and refocusing by the composite of two successive β pulses. For stimulated echoes, the magnetization vector is stored in the longitudinal direction in between the two β pulses and, thus, the gradient has no effect on the phase distribution. The resultant 1-(-1) waveform (dotted-dashed areas, respectively) shows no inherent motion compensation. Note that, with flip angle reduction of the β pulses, as with the selection of the TRF pulse, the signals have a decreased contribution from the spin echo and increases the stimulated echo portion. Therefore, the noncompensated stimulated echo reduces the high-intensity CSF artifacts due to rapid inflow of CSF in the prepontine cisterns.

the velocity is much lower (on the order of 5–10 cm/s) than that in the major blood vessels. The effectiveness of inflow saturation to reduce high-intensity CSF artifacts, therefore, is anticipated to be limited, as shown in Tables 2 and 3.

Similar to inflow saturation, the results from this study indicate that section FC did not significantly influence the quality of fast-FLAIR images. One possible reason is that the signals in fast spin-echo sequences are inherently motion-compensated at even echoes along the section direction (19) (Fig 2A), hence yielding no discernible difference with further addition of the through-plane FC gradients. The ineffectiveness of additional section FC in fast spin-echo sequences is expected to be especially prominent when the flow is slow and does not contain a substantial portion of higher-order flow acceleration, as in the case of CSF motion. Also note that, although findings in the volunteer study showed that fast-FLAIR images obtained with section FC, TRF, and three interleaving acquisitions had the best image quality, FC is not thought to play an essential role in reducing the artifacts because of two reasons: First, because of the imaging time, we did not perform imaging in the volunteers by using TRF pulses and three interleaving acquisitions without FC (Table 3) for a comprehensive comparison. Second, as have already been stated, results from the patient study suggested that FC did not significantly alter the incidence of high-intensity CSF artifacts.

The reason why TRF helped to suppress non-nullified CSF signals is anticipated to be associated with the formation of stimulated echoes in fast spin-echo sequences. To appreciate this point, note first that two major components contribute to the received signals in fast spin-echo sequences: spin echoes and stimulated echoes (Fig 2). In contrast to spin echo that arises from one excitation RF pulse followed by one refocusing pulse, the stimulated echo is formed by three consecutive RF pulses: The first one serves as the excitation pulse, whereas the latter two serve as a composite refocusing pulses. Along the section-selection direction, the spin echoes are inherently motion compensated at even echoes (Fig 2A) (19), whereas the stimulated echoes are not (Fig 2B). This is because the gradient experienced by the magnetization vector exhibits a 1-(-2)-1 waveform (ie, the gradient waveform for FC) at even spin echoes (20). On the other hand, the stimulated echoes experience only a 1-(-1) waveform (similar to that of common gradient-echo imaging); hence, they are not motion compensated (Fig 2B). Consequently, for through-plane flow, strong signals are expected for the spin echoes, whereas the stimulated echoes experience intravoxel phase dispersion leading to signal loss (21). The TRF technique is a method that was originally developed to stabilize fast spin-echo signal amplitudes (12), including those in fast-FLAIR. The design involves varying the flip angles of the first two refocusing pulses, along with a flip-angle reduction for the remaining ones. Compared with standard fast spin-echo with 180° refocusing pulses, the reduction of the flip angle in the TRF method decreases the spin-echo contribution to the signals and concomitantly increases the stimulated echo portion (22). In other words, selection of the TRF option in the fast-FLAIR sequence had the effect of increasing the stimulated echo, whereas no significant visible change occurred on T2-weighted image. Because the high-intensity CSF artifacts at the basal cisterns on fast-FLAIR images come predominantly from the through-plane motion that causes non-nullified CSF, these artifactual signals are optimally be dephased with the use of the noncompensated stimulated echoes. The results from this study suggest that the selection of TRF in fast-FLAIR imaging had the effect of increased stimulated-echo components, which achieved effective CSF suppression. One further note is that the TRF mentioned in this study refers to the echo amplitude stabilization scheme proposed by Le Roux and Hinks (12), and it should not be confused with the same terminology used to described RF pulses with a quadratic phase distribution within the selected section (23).

Another effective method to prevent inflow of non-inverted CSF into the image section is to increase the thickness of the inversion pulse. This change can be accompanied by an increased intersection gap to min-

imize possible "cross-talking" between adjacent inversion pulses. When the intersection gap is not desirable, the image acquisition must be interleaved, at the penalty of a longer imaging time. For contiguous sections with an interleaving acquisition factor of *N*, the thickness of the inversion pulse can be increased to approximately *N* times the image section; this is exactly the recommendation of the manufacturer of the MR system that was used in this study. The increase in the inversion section thickness thus accounts for the better CSF suppression at the basal cisterns noted in this study when we increased the interleaving acquisition factor from 2 to 3. However, in this study, changing the interleaving acquisition factor from 2 to 3 increased the imaging time from 4 minutes 42 seconds to 7 minutes 3 seconds; this increase may not be favorable in busy clinical settings.

We did not investigate the effects of cardiac gating as a potential method to reduce high-intensity CSF artifacts. In fact, even with the knowledge that CSF motion is driven by cardiac pulsation (24), the usual implementation of cardiac gating to synchronize image acquisition is not anticipated to help in reducing the high-intensity CSF artifacts at fast-FLAIR imaging. To elucidate this point, note that two approaches to cardiac gating are generally used. The first is to synchronize image acquisition with the cardiac cycle, and the second is to perform FLAIR readout during diastole of the cardiac cycle. Both methods are expected to minimize amplitude fluctuations of the received signals along the phase-encoding direction. Therefore, motion ghosts along the phase-encoding direction could be reduced to a minimum with cardiac gating. However, neither of these gating approaches is related to the inflow of noninverted CSF into the imaging section that occurs during the 2-second TI. Hence, cardiac gating should not be used to reduce high-intensity CSF artifacts and does not need to be compatible with the fast-FLAIR technique, as is the case for the MR system used in our study.

If cardiac gating is implemented in a way to reduce high-intensity CSF artifacts at fast-FLAIR imaging, the separation of the inverting 180° and excitation 90° pulses should be synchronized (ie, TI equal to an integer multiple of the cardiac cycle). Although this approach is possible, it is complicated by the following: 1) Changes in TI itself may lead to imperfect nulling of the CSF signal (17), which creates more high-intensity CSF artifacts, even for nonmoving CSF; and 2) multisection interleaving within TI becomes less flexible when TI changes all the time. On the other hand, if the CSF signal can be appropriately suppressed, motion ghosts would also have zero signal intensity and, hence, not be a problem at all. As a result, the fact that the manufacturer of our MR system does not implement cardiac gating with the fast-FLAIR sequence seems fully comprehensible.

One final note is that the influence of the imaging parameters investigated in this study is specifically restricted to fast-FLAIR imaging with selective inversion. Recent studies (25–27) have involved the use of nonselective inversion pulses for an effective elimination of high-intensity CSF artifacts at the expense of altered image contrast (25), which is correctable with a k-space reordering scheme (26, 27). In FLAIR with nonselective inversion, a single inversion pulse was used in all imaging sections, whereas in FLAIR with selective inversion, one inversion pulse was used for each imaging section. Because of intrinsically different inversion schemes, effects of imaging parameters on high-intensity CSF artifacts, as found in our study, do not apply to the FLAIR sequence with nonselective inversion. By the same token, the k-space reordering technique to improve image quality (26, 27) is irrelevant to the fast-FLAIR method investigated in this study. On the other hand, the use of adiabatic inversion pulse to correct an imperfect pulse profile at the edge of the RF coil (28) can theoretically be directly applied to the fast-FLAIR sequence used in our study to further improve the suppression of CSF signals.

Our findings suggest that, even with our preferred choice of TRF and two interleaving acquisitions in the routine clinical application of fast-FLAIR imaging, the incidence of high-intensity CSF artifacts at the basal cisterns (>40%, Table 1) is still notable. Although most aneurysmal subarachnoid hemorrhages occur in the suprasellar cisterns, where the high incidence of artifacts does not seem to be a problem because CSF suppression remains largely successful in this area. Approximately 10% of the cases with subarachnoid hemorrhage from aneurysms in the basilar system occur as isolated prepontine hemorrhage (29). Therefore, the possibility that the high-intensity CSF artifacts on fast-FLAIR images can obscure hemorrhagic lesions should be given special attention, particularly so with subacute subarachnoid hemorrhages in which the fast-FLAIR signal intensity may not be as high as that in the acute lesion (10).

Conclusion

The findings of this study showed that high-intensity CSF artifacts at the basal cisterns occur at a rate of about 40–80% on fast-FLAIR images. They are frequently encountered in the presence of rapid CSF flow and may obscure hemorrhagic lesions. The appropriate choice of optional sequence parameters in fast-FLAIR imaging helps reduce the incidence of artifacts.

References

1. De Coene B, Hajnal JV, Gatehouse P, et al. **MR of the brain using fluid-attenuated inversion recovery (FLAIR) pulse sequences.** *AJNR Am J Neuroradiol* 1992;13:1555–1564
2. Tsuchiya K, Mizutani Y, Hachiya J. **Preliminary evaluation of fluid-attenuated inversion-recovery MR in the diagnosis of intracranial tumors.** *AJNR Am J Neuroradiol* 1996;17:1081–1086
3. Bakshi R, Kamran S, Kinkel PR, et al. **Fluid-attenuated inversion-recovery MR imaging in acute and subacute cerebral intraventricular hemorrhage.** *AJNR Am J Neuroradiol* 1999;20:629–636
4. Hajnal JV, Bryant DJ, Kasuboski L, et al. **Use of fluid attenuated inversion recovery (FLAIR) pulse sequences in MRI of the brain.** *J Comput Assist Tomogr* 1992;16:841–844
5. Noguchi K, Ogawa T, Inugami A, et al. **Acute subarachnoid hemorrhage: MR imaging with fluid-attenuated inversion recovery**

pulse sequences. *Radiology* 1995;196:773–777
6. Brant-Zawadzki M, Atkinson D, Detrick M, et al. **Fluid-attenuated inversion recovery (FLAIR) for assessment of cerebral infarction: initial clinical experience in 50 patients.** *Stroke* 1996;27:1187–1191
7. Singer MB, Atlas SW, Drayer BP. **Subarachnoid space disease: diagnosis with fluid-attenuated inversion-recovery MR imaging and comparison with gadolinium-enhanced spin-echo MR imaging—blinded reader study.** *Radiology* 1998;208:417–422
8. Rydberg JN, Hammond CA, Grimm RC, et al. **Initial clinical experience in MR imaging of the brain with a fast fluid-attenuated inversion-recovery pulse sequence.** *Radiology* 1994;193:173–180
9. Tsuchiya K, Inaoka S, Mizutani Y, Hachiya J. **Fast fluid-attenuated inversion-recovery MR of intracranial infections.** *AJNR Am J Neuroradiol* 1997;18:909–913
10. Noguchi K, Ogawa T, Seto H, et al. **Subacute and chronic subarachnoid hemorrhage: diagnosis with fluid-attenuated inversion-recovery MR imaging.** *Radiology* 1997;203:257–262
11. Adams JG, Melhem ER. **Clinical usefulness of T2-weighted fluid-attenuated inversion recovery MR imaging of the CNS.** *AJR Am J Roentgenol* 1999;172:529–536
12. Le Roux P, Hinks RS. **Stabilization of echo amplitudes in FSE sequences.** *Magn Reson Med* 1993;30:183–191
13. Melhem ER, Jara H, Eustace S. **Fluid-attenuated inversion recovery MR imaging: identification of protein concentration thresholds for CSF hyperintensity.** *AJR Am J Roentgenol* 1997;169:859–862
14. Essig M, Hawighorst H, Schoenberg SO, et al. **Fast fluid-attenuated inversion-recovery (FLAIR) MRI in the assessment of intraaxial brain tumors.** *J Magn Reson Imaging* 1998;8:789–798
15. Waga S, Shimosaka S, Sakakura M. **Intracerebral hemorrhage remote from the site of the initial neurosurgical procedure.** *Neurosurgery* 1983;13:662–665
16. Bakshi R, Caruthers SD, Janardhan V, Wasay M. **Intraventricular CSF pulsation artifact on fast fluid-attenuated inversion recovery MR images: analysis of 100 consecutive normal studies.** *AJNR Am J Neuroradiol* 2000;21:503–508
17. Rydberg JN, Riederer SJ, Rydberg CH, Jack CR. **Contrast optimization of fluid-attenuated inversion recovery (FLAIR) imaging.** *Magn Reson Med* 1995;34:868–877
18. Melhem ER, Jara H, Shakir H, Gagliano TA. **Fast inversion-recovery MR: the effect of hybrid RARE readout on the null points of fat and cerebrospinal fluid.** *AJNR Am J Neuroradiol* 1997;18:1627–1633
19. Katz J, Peshock RM, Malloy CR, Schaeffer S, Parkey RW. **Even-echo rephasing and constant velocity flow.** *Magn Reson Med* 1987;4:422–430
20. Haacke EM, Lenz GW. **Improving image quality in the presence of motion by using rephasing gradients.** *AJR Am J Roentgenol* 1987;148:1251–1258
21. Hinks RS, Constable RT. **Gradient moment nulling in fast spin echo.** *Magn Reson Med* 1994;32:698–706
22. Hennig J. **Multiecho imaging sequences with low refocusing flip angles.** *J Magn Reson* 1988;78:397–407
23. Cho ZH, Ro YM. **Reduction of susceptibility artifact in gradient-echo imaging.** *Magn Reson Med* 1992;23:193–200
24. Bradley WG Jr, Scalzo D, Queralt J, Nitz WN, Atkinson DJ, Wong P. **Normal-pressure hydrocephalus: evaluation with cerebrospinal fluid flow measurements at MR imaging.** *Radiology* 1996;198:523–529
25. Tanaka N, Abe T, Kojima K, Nishimura H, Hayabuchi N. **Applicability and advantages of flow artifact-insensitive fluid-attenuated inversion-recovery MR sequences for imaging the posterior fossa.** *AJNR Am J Neuroradiol* 2000;21:1095–1098
26. Herlihy AH, Oatridge A, Curati WL, Puri BK, Bydder GM, Hajnal JV. **FLAIR imaging using nonselective inversion pulses combined with slice excitation order cycling and k-space reordering to reduce flow artifacts.** *Magn Reson Med* 2001;46:354–364
27. Herlihy AH, Hajnal JV, Curati WL, et al. **Reduction of CSF and blood flow artifacts on FLAIR images of the brain with k-space reordered by inversion time at each slice position (KRISP).** *AJNR Am J Neuroradiol* 2001;22:896–904
28. Hajnal JV, Oatridge A, Herlihy AH, Bydder GM. **Reduction of CSF artifacts on FLAIR images by using adiabatic inversion pulses.** *AJNR Am J Neuroradiol* 2001;22:317–322
29. Kallmes DF, Clark HP, Dix JE, et al. **Ruptured vertebrobasilar aneurysms: frequency of the nonaneurysmal perimesencephalic pattern of hemorrhage on CT scans.** *Radiology* 1996;201:657–660